
Information Bottleneck Theory on Convolutional Neural Networks

JunjieLi · DingLiu

Received: date / Accepted: date

Abstract Recent years, many researches attempt to open the black box of deep neural networks and propose a various of theories to understand it. Among them, Information Bottleneck (IB) theory claims that there are two distinct phases consisting of fitting phase and compression phase in the course of training. This statement attracts many attentions since its success in explaining the inner behavior of feedforward neural networks. In this paper, we employ IB theory to understand the dynamic behavior of convolutional neural networks (CNNs) and investigate how the fundamental features such as convolutional layer width, kernel size, network depth, pooling layers and multi-fully connected layer have impact on the performance of CNNs. In particular, through a series of experimental analysis on benchmark of MNIST and Fashion-MNIST, we demonstrate that the compression phase is not observed in all these cases. This shows us the CNNs have a rather complicated behavior than feedforward neural networks.

Keywords Information Bottleneck · Convolutional Neural Networks · Deep Learning · Representation Learning

1 Introduction

In recent, the practical successes of deep neural networks have generated many attempts to explain the performance of deep learning [11, 14, 33], especially in terms of the dynamics of the optimization [1, 21]. In this context, the Information Bottleneck (IB) theory provides a fundamental tool on this topic, and some preliminary empirical exploration of these ideas in deep feedforward neural networks has yielded striking findings [2, 8, 19, 23, 28]. Besides, people start to investigate IB theory from different perspective such as gaussian variables [3, 18], multivariate systems [6], hidden variable networks [5], nonlinear systems [16], neural network-based classification [2], compression of neural networks [4], even for the application of document clustering [24] and video search reranking [12]. Moreover, Ref. [7, 25] discuss the entropy and mutual information in more detail, and Ref. [22] proves several finite sample bounds which show that information bottleneck can provide representations with good generalization. In addition, Ref. [13] presents Mutual Information Neural Estimation (MINE) that can stabilize the test accuracy and reduce its variance.

Inspired from these works, we investigate the IB theory using an analytical method on Convolutional Neural Networks (CNNs), which have wide application on such as image processing in recent years [29, 30]. And we observe quite different behaviors in contrast to those of feedforward neural networks. In the series of original works [23, 27, 28], authors hold some core points that the distinct phases of the Stochastic Gradient Descent (SGD) optimization, drift and diffusion, which explain the empirical error minimization and the representation compression trajectories of the layers. These phases are characterized by very different signal to noise ratios of the stochastic gradients in every layer. This funding opens the black box of deep learning from the perspective

JunjieLi

Department of Computer Science and Technology, School of Computer Science and Technology, Tiangong University, Tianjin 300387, China

DingLiu

Department of Computer Science and Technology, School of Computer Science and Technology, Tiangong University, Tianjin 300387, China E-mail: liuding@tiangong.edu.cn

of information theory and draw many attentions. Along this way, a further research offers some different views of IB theory and shows us some different behaviors on feedforward neural networks [20]. They say that “fitting” and “compression” phases in the course of training strongly depend on the nonlinear activation. The authors state that double saturating nonlinearities lead to compression and stochasticity in the training phase does not contribute to compression. Obviously, it is partly in contradiction with the initial idea in Ref. [23]. Moreover, Ref. [7] claims that the compression can happen even when using ReLu activation in their high dimensional experiments, and there is not a clear link between compression and generalization. Then lately, some works start to focus on exploring the inner organization of CNNs and autoencoders by using matrix-based Renyi’s entropy [31, 32]. The authors propose that variability in the compression behavior strongly depends on different estimators. By using matrix-based Renyi’s entropy estimator and remove the redundant information in the MI, they observe compression phase during the training. Moreover, Ref. [9] find a new phenomenon – clustering emerging in the training phase. And they propose that the compression strongly rely on the clustering and may not causally related to generalization. So until now, based on all these previous works, compression and the relationship between it and generalization still remain elusive.

In this paper, different from the previous works, we observe no compression phase both on convolution layers and fully connected layers on standard CNNs, even with double saturating nonlinearity such as *tanh*. This observation partly supports the conclusion by Ref. [20] that compression is not the universal phase during the course of training. Moreover, from the perspective of IB theory, we investigate how the fundamental features such as convolutional layer width, network depth, kernel size, pooling layers etc. have an effect on the performance of CNNs. The experimental results verify the importance of these features in improving the generalization performance.

2 Method

The Information Bottleneck (IB) theory is introduced by Tishby et.al first time in the paper [27]. Afterwards, Ref. [23, 28] analyse the training phase of Deep Neural Networks (DNNs) from the perspective of IB. Accordingly, IB suggests that each hidden layer will capture more useful information from the input variable, and the hidden layers are supposed to be the maximally compressed mappings of the input. There are several fundamental points to know about IB theory as follow:

2.1 Mutual Information

Mutual Information (MI) measures the mutual dependence of two random variables. Further, it quantifies the amount of information got about one random variable through observing the other. For example, given two variables A and B , mutual information $I(A; B)$ is defined as:

$$I(A; B) = H(A) - H(A|B) \quad (1)$$

$$H(A) = - \sum_{a \in A} p(a) \log p(a) \quad (2)$$

$$\begin{aligned} H(A|B) &= - \sum_{b \in B} p(b) \sum_{a \in A} p(a|b) \log p(a|b) \\ &= - \sum_{a \in A} \sum_{b \in B} p(b, a) \log p(a|b) \end{aligned} \quad (3)$$

where $H(A)$ and $H(A|B)$ are entropy and conditional entropy respectively, and $p(b, a)$ denotes joint probability distribution.

2.2 Binning-based MI Estimator

The binning-based MI estimator is widely used in feedforward neural networks. And as we know, CNNs are characterized as sparse interactions (sparse connectivity) in compare with feedforward neural networks as

shown in Fig. 1, which appears in Ref. [10]. In principle, the sparsity will not lead to the failure of binning-based estimator. So along this way, we also use it to evaluate the MI in CNNs. First, we reshape the output images of each channel of each convolutional layer into a vector, and splice these vectors into a long one h . Then, according to Ref. [20], we discretize the activation output by a fixed bin size, i.e. $T = \text{bin}(h)$. (Ref. [20] choose 0.5, while in this paper, we use the constant 0.67 as bin size. Because according to our experimental results, it is good for visualization and meets the results of kernel density estimation method in [15, 16].) We show the process in Fig. 2.

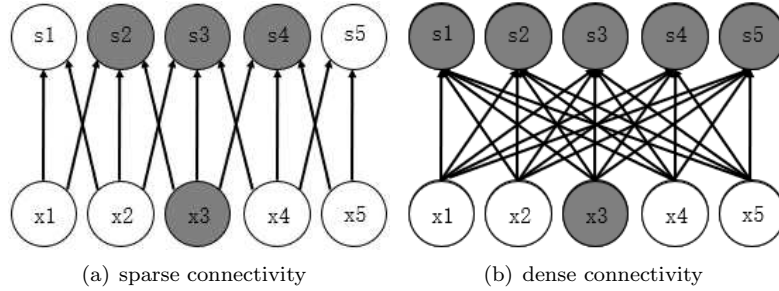


Fig. 1 Sparse connectivity and dense connectivity (fully connected) .

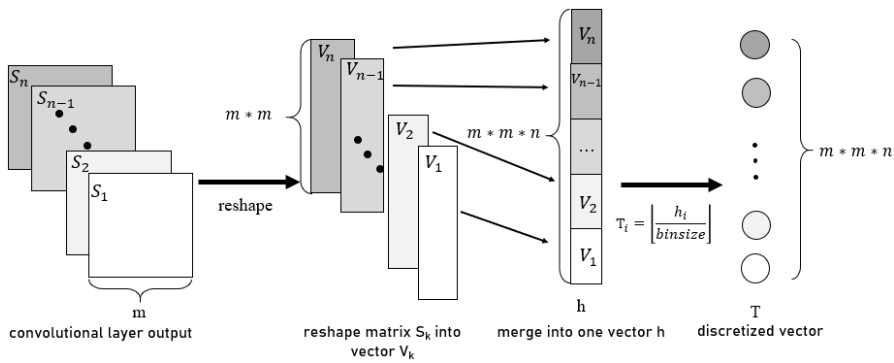


Fig. 2 The process of binning activity. Each channel of layer's output is firstly converted into a vector, and then these vectors are combined into a long one, i.e. h . Then, it is mapped into a new vector by dividing by the constant bin size.

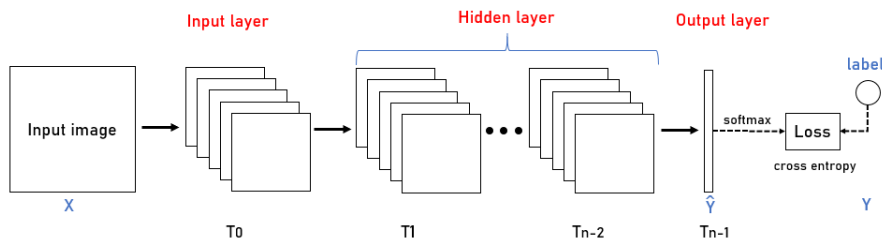
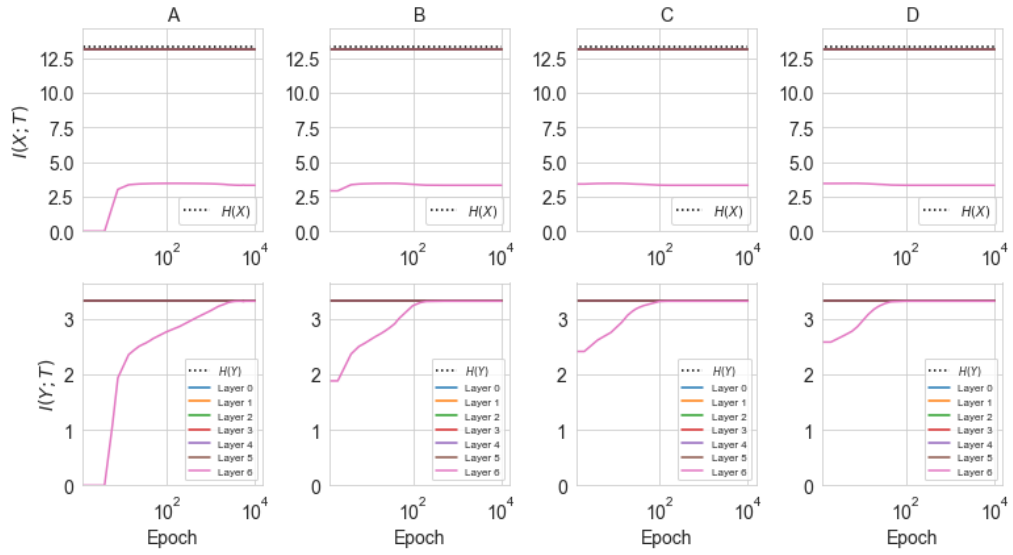


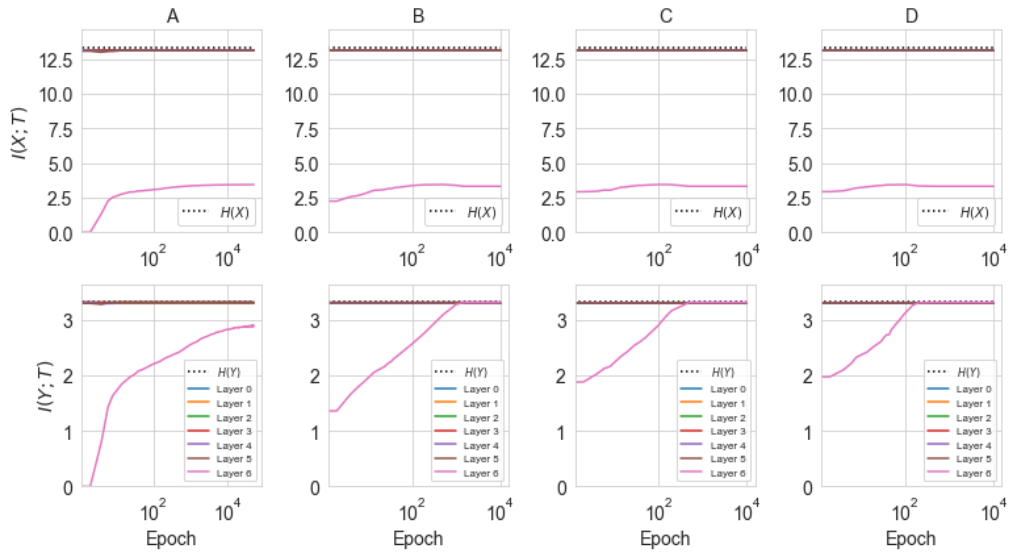
Fig. 3 Architecture of our convolutional network model. X denotes the input data and Y is the label.

T_0 is input layer. $T_0 \sim T_{n-2}$ are convolutional layers. T_{n-1} is fully connected output layer.

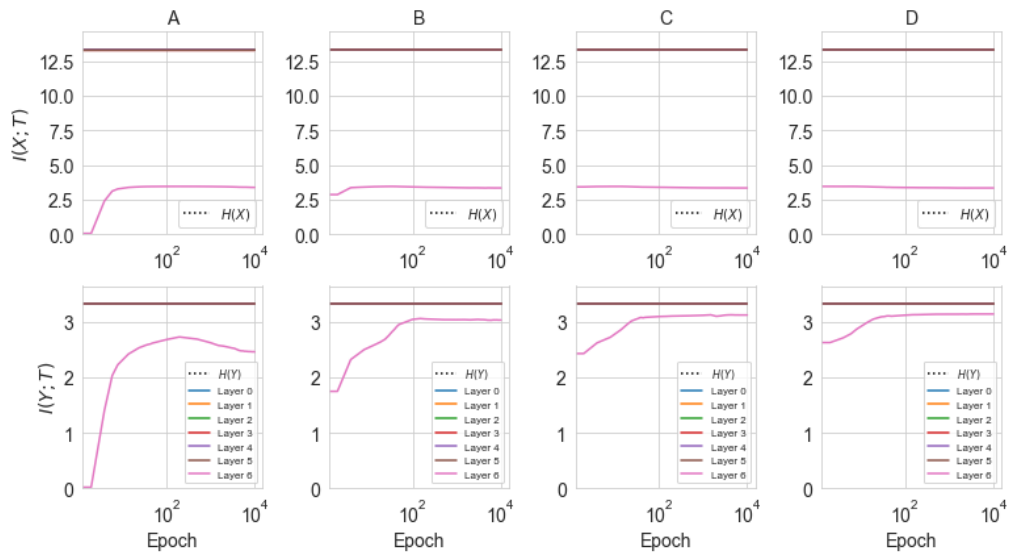
In this case, we use the fact that $H(T|X) = 0$ (We treat every input data and the output of each layer as a vector variable respectively. Because of the high dimension of the input variable, each input data will



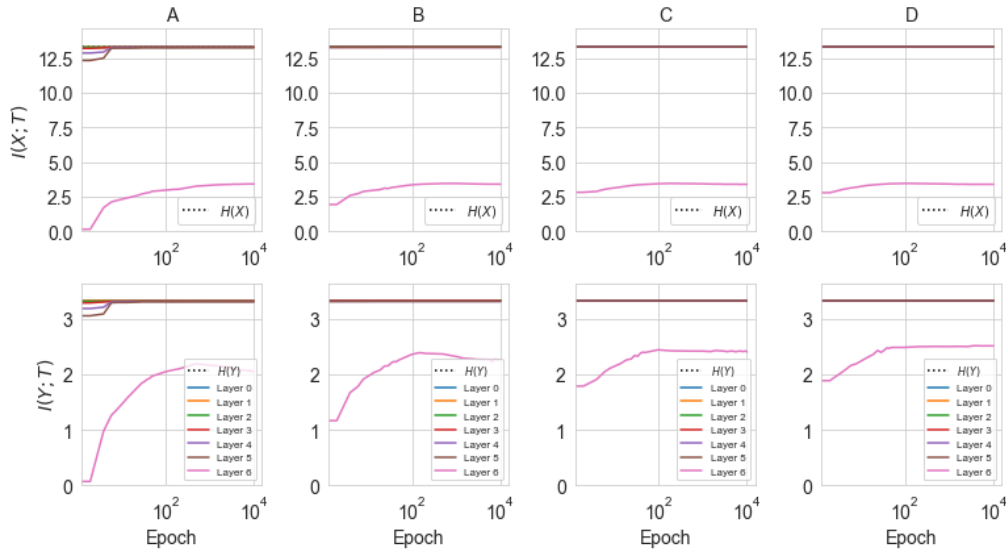
(a) MI path on training data of MNIST



(b) MI path on training data of Fashion-MNIST



(c) MI path on test data of MNIST



(d) MI path on test data of Fashion-MNIST

Fig. 4 (Colored online) MI path on CNNs with different convolutional layer widths. Colored lines mark each layer of network. As we describe in *Experiments and discussion* section, layer 0 ~ 5 are convolutional layers, and layer 6 is final output layer (fully connected layer). In this experiment, layer 0 matches layer T_0 in Fig. 3, layer 5 matches layer T_{n-2} in Fig. 3 and layer 6 matches layer T_{n-1} in Fig. 3.

Convolutional layer 5 (the final convolutional layer) covers all previous layers, $H(X)$ and $H(Y)$ since they all have the same value. The convolutional layer width of 4 networks are (A) 1-1-1-1-1-1, (B) 3-3-3-3-3-3, (C) 6-6-6-6-6-6, (D) 12-12-12-12-12-12. The pink line represents the mutual information of final output layer, which grows until getting stable as the process of training. The kernel size of these networks are set to 3x3.

correspond to a output of every layer. So the conditional entropy is equal to zero). Then $I(T; X)$ and $I(T; Y)$ can be rewritten respectively as:

$$\begin{aligned}
 I(T; X) &= H(T) - H(T|X) \\
 &= H(T) \\
 &= -\sum_{i=1}^n p_i \log p_i
 \end{aligned} \tag{4}$$

$$\begin{aligned}
 I(T; Y) &= H(T) - H(T|Y) \\
 &= -\sum_{i=1}^n p_i \log p_i + \sum_{i=1}^n p_i H(T|Y = y_i)
 \end{aligned} \tag{5}$$

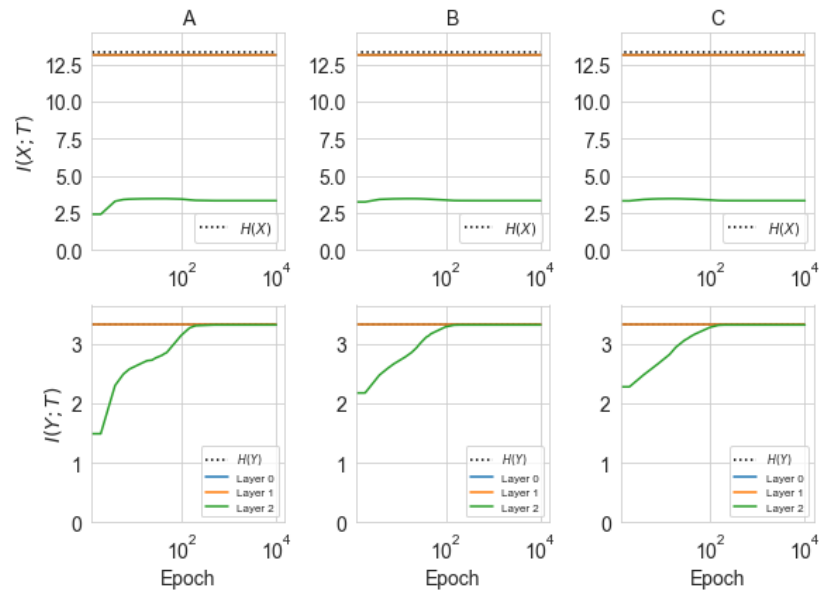
where p_i is the probability that an activation output lands in the i th interval.

2.3 Information Plane And Data Processing Inequality

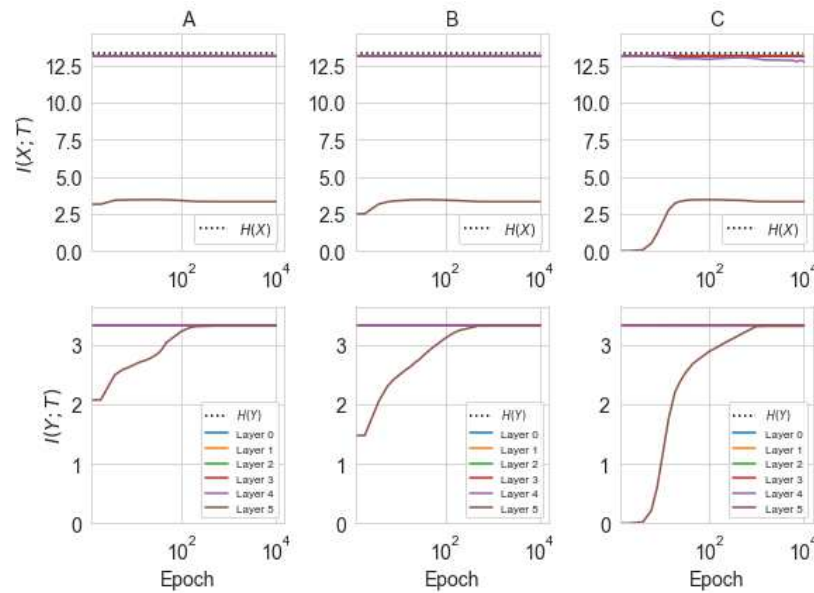
Information plane (IP) shows the dynamic behavior of $I(Y; T)$ with respect to $I(X; T)$ [23]. They propose that the optimization of feedforward neural networks involve two phases, namely fitting phase and compression phase. In the fitting phase, the feedforward neural networks try to fit training samples into corresponding labels by increasing both $I(X; T)$ and $I(Y; T)$. In compression phase, the feedforward neural networks discard redundant information by reducing $I(X; T)$. Based on these statements, people will observe these two apparent phases on IP.

Moreover, the MI among all feedforward neural networks layers form a Markov chain, which leads to Data Processing Inequality (DPI). It can be depicted as:

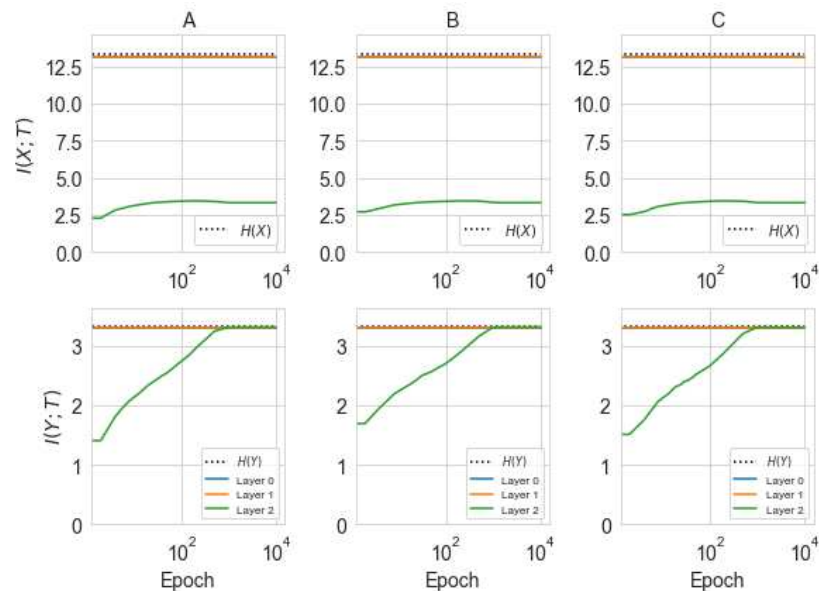
$$\begin{aligned}
 H(X) &\geq I(X; T_0) \cdots I(X; T_{n-2}) \geq I(X; T_{n-1}) \\
 H(Y) &\geq I(Y; T_0) \cdots I(Y; T_{n-2}) \geq I(Y; T_{n-1})
 \end{aligned} \tag{6}$$



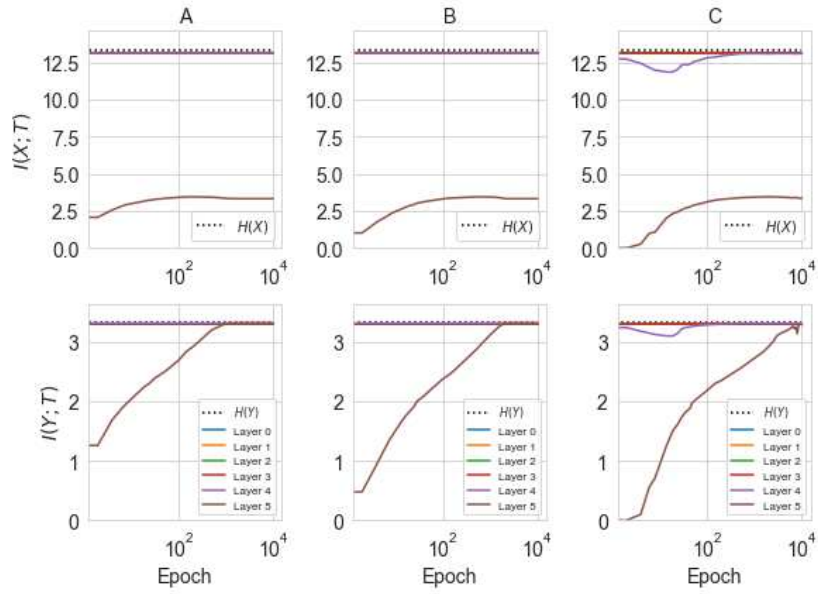
(a) MI path on training data of MNIST. All networks with fixed depth = 3. The sizes of kernel are (A) 3×3 (B) 7×7 (C) 11×11



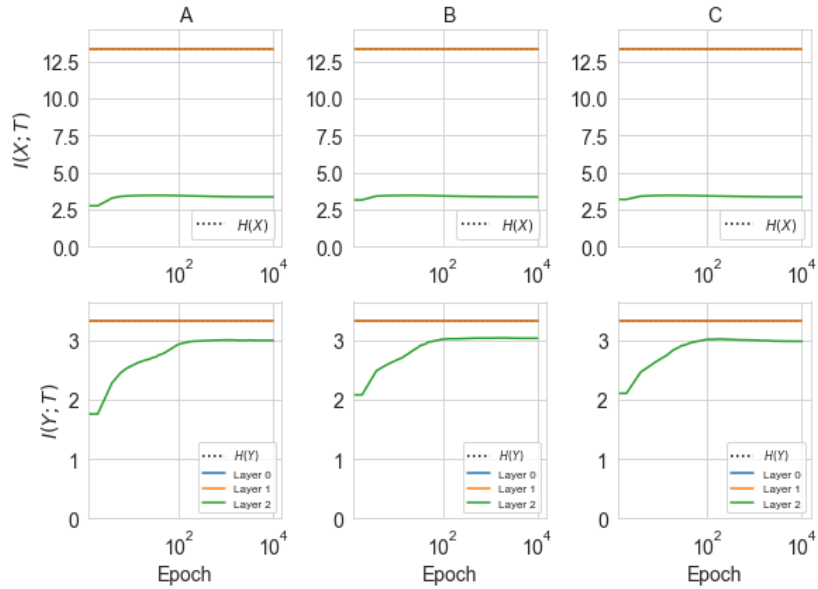
(b) MI path on training data of MNIST. All networks with fixed depth = 6. The sizes of kernel are (A) 3×3 (B) 5×5 (C) 7×7



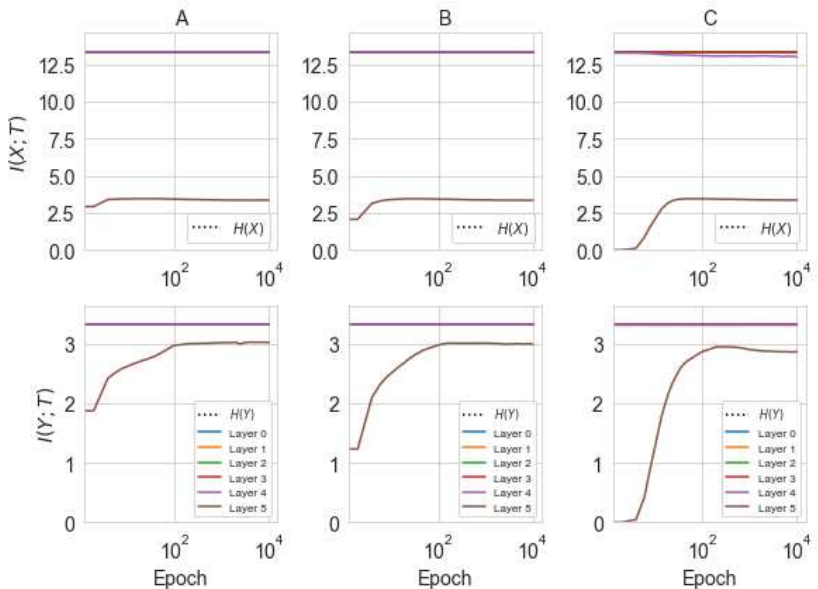
(c) MI path on training data of Fashion-MNIST. All networks with fixed depth = 3. The sizes of kernel are (A) 3×3 (B) 7×7 (C) 11×11



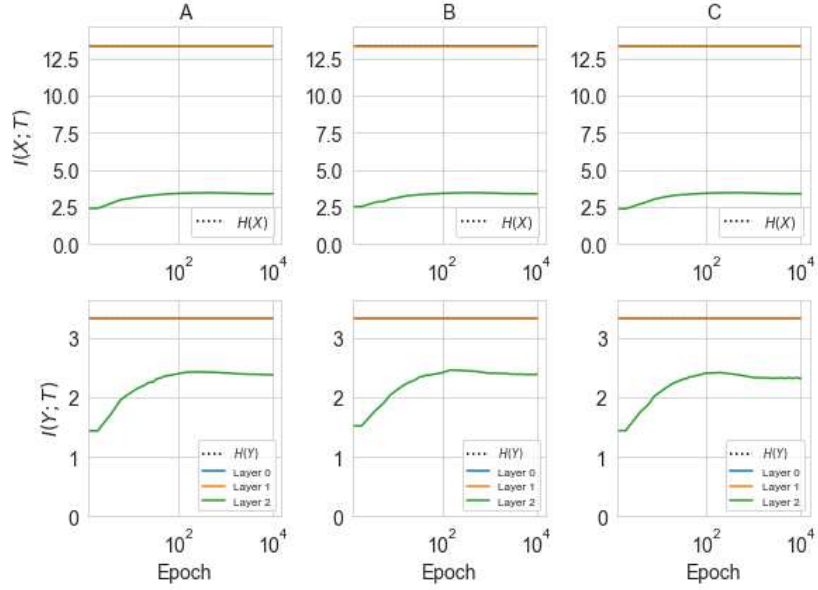
(d) MI path on training data of Fashion-MNIST. All networks with fixed depth = 6. The sizes of kernel are (A) 3 x 3 (B) 5 x 5 (C) 7 x 7



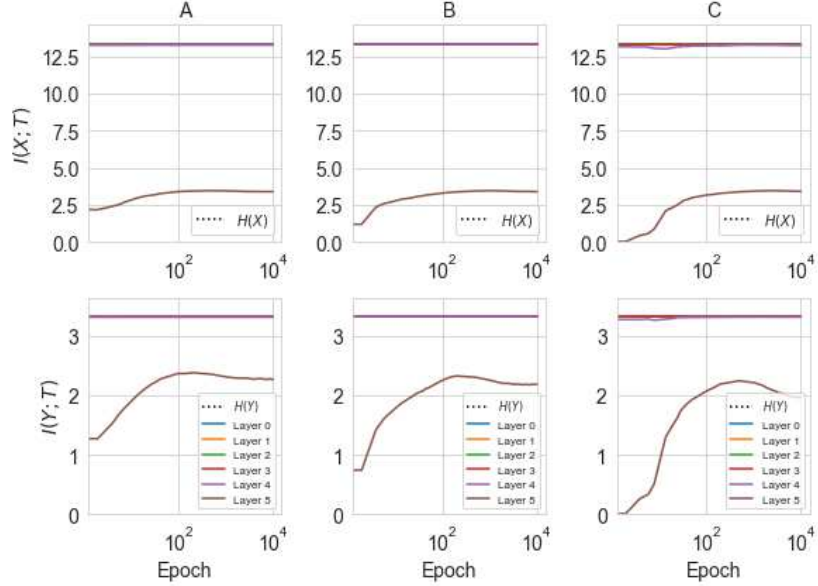
(e) MI path on test data of MNIST. All networks with fixed depth = 3. The sizes of kernel are (A) 3 x 3 (B) 7 x 7 (C) 11 x 11



(f) MI path on test data of MNIST. All networks with fixed depth size = 6. The sizes of kernel are (A) 3 x 3 (B) 5 x 5 (C) 7 x 7



(g) MI path on test data of Fashion-MNIST. All networks with fixed depth = 3. The sizes of kernel are (A) 3×3 (B) 7×7 (C) 11×11



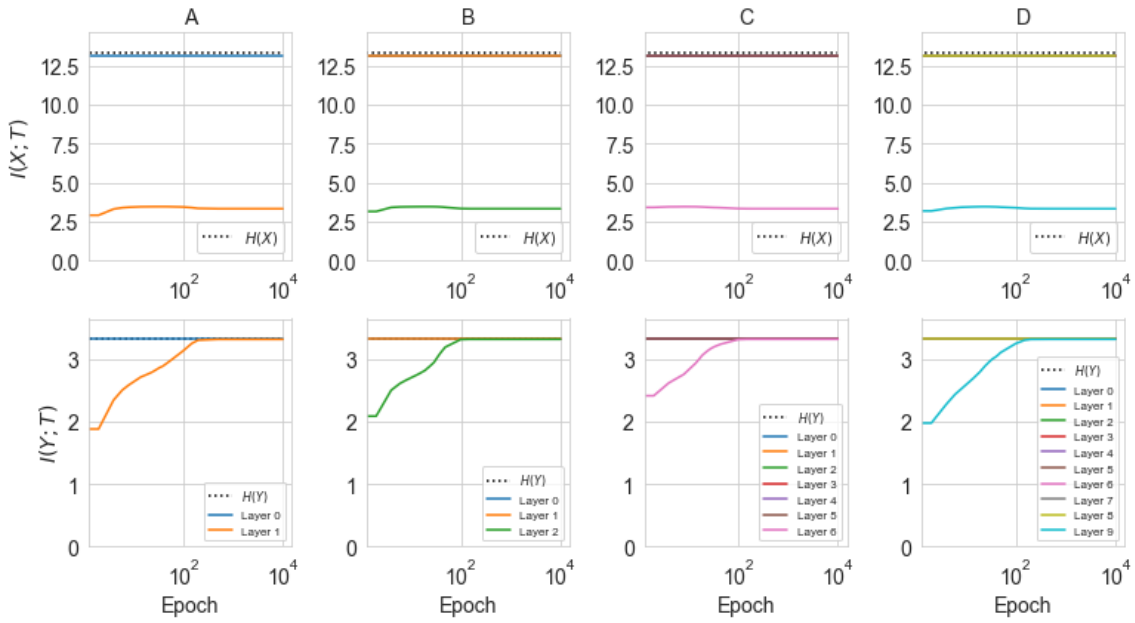
(h) MI path on test data of Fashion-MNIST. All networks with fixed depth = 6. The sizes of kernel are (A) 3×3 (B) 5×5 (C) 7×7

Fig. 5 (Colored online) MI path on CNNs with different convolutional kernel sizes. In this configuration, all convolutional layers width are set to 3.

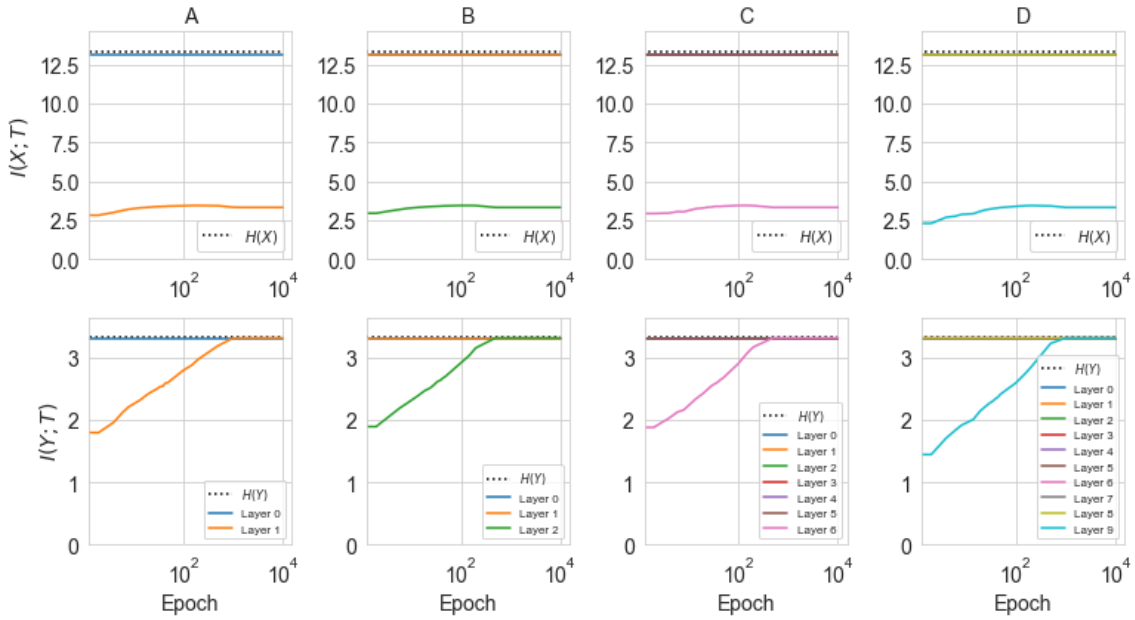
where T_0 is input layer, $T_1 \cdots T_{n-2}$ are hidden layers, and T_{n-1} denotes the final output layer.

3 Experiments and discussions

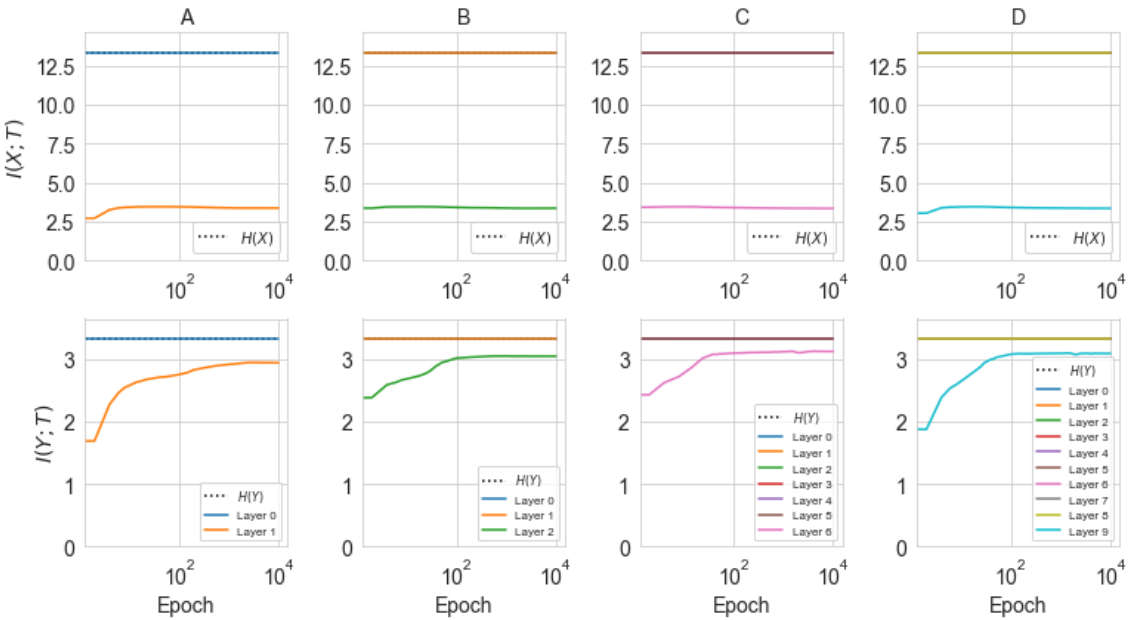
In order to investigate the impact of IB theory on CNNs, we perform a series of experiments on MNIST and Fashion-MNIST datasets which are two popular benchmarks on image classification. The training set consists of 60 000 (28×28) gray-scale images, with 10 000 testing examples. For simplicity, we select 10,000 training samples randomly as training dataset and 10,000 test samples as test dataset. The networks are trained by using Adam algorithm and cross-entropy loss function with batch of 1000 samples. In addition, we set the learning rate as 10^{-3} , and use *tanh* activation except for final output layer with softmax. Our model is shown



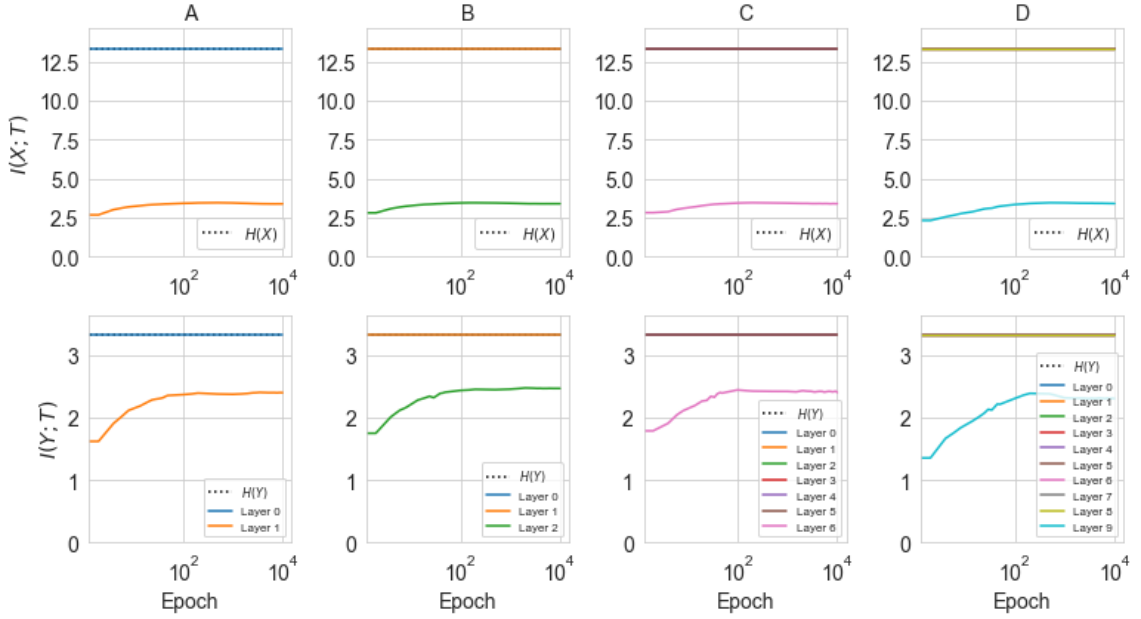
(a) MI path on training data of MNIST. (A) depth=2, (B) depth=3, (C) depth=7, (D) depth=10



(b) MI path on training data of Fashion-MNIST. (A) depth=2, (B) depth=3, (C) depth=7, (D) depth=10



(c) MI path on test data of MNIST. (A) depth=2, (B) depth=3, (C) depth=7, (D) depth=10



(d) MI path on test data of Fashion-MNIST. (A) depth=2, (B) depth=3, (C) depth=7, (D) depth=10

Fig. 6 (Colored online) MI path on CNNs with different depths. All width of convolutional layers are 6, and all kernel sizes are set to 3×3 .

in Fig. 3. The MI is evaluated on both training dataset and test dataset respectively. Therefore, in this case, $H(X)$ for both training dataset and test dataset equals to $\log_2 10^4$. Then, we analyse the impact of some crucial features such as convolutional layer width, network depth, kernel size and pooling layer on CNNs from view point of IB theory. Specifically, we discuss the compression phase on CNNs architecture. Our code is available on the Github.com¹. The detailed information on these two benchmarks could be found at the official website: (<http://yann.lecun.com/exdb/mnist/>) and (<https://github.com/zaladoresearch/fashion-mnist>).

3.1 Convolutional Layer Width

The convolutional layer width is crucial on the way to understand representation power of neural networks. To study the effect of convolutional layer width from the perspective of IB theory, we train 4 different CNNs with various of convolutional layer widths (number of channels).

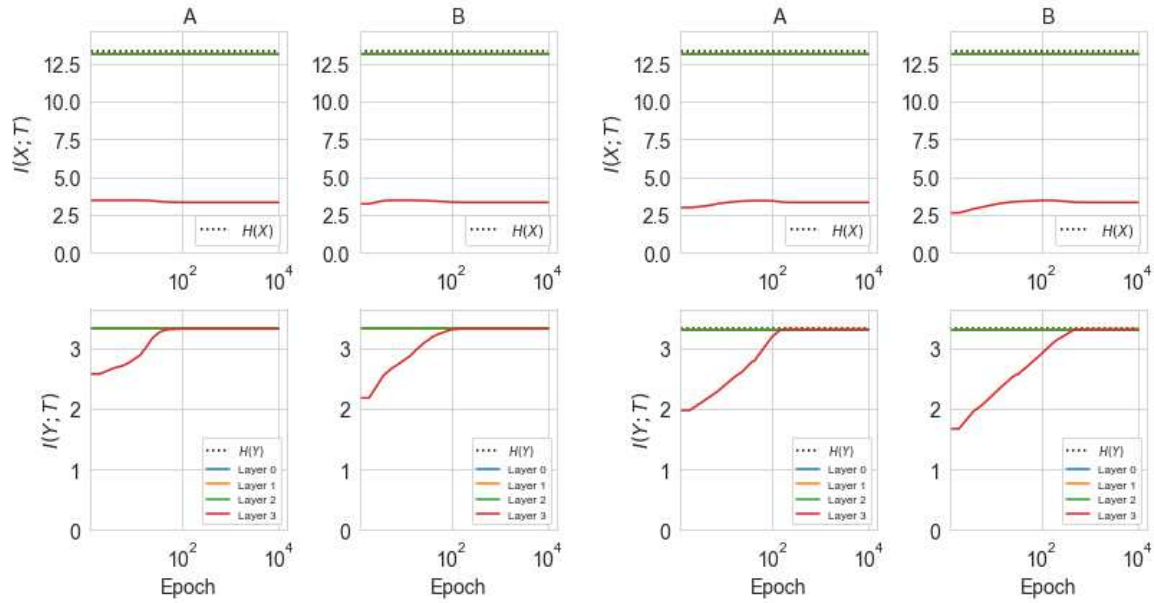
Fig. 4 shows the $I(Y; T)$ and $I(X; T)$ paths on these networks during the training and test phase. By using DPI we introduce earlier, the theoretical upper bound of $I(X; T)$ of each layer is $H(X)$. Similarly, the theoretical upper bound of $I(Y; T)$ equals to $H(Y)$. Therefore, in this figure, we observe the MI on all convolutional layers reach the upper bound which means they capture almost all information on input X and label Y . This is due to we treat the whole image as a single variable, then all images are basically different. So according to Eq. 4, $I(X; T)$ can be represented by $H(T)$. Moreover, $H(T)$ is equal to $\log_2 10^4$ i.e. $H(X)$. In the same view, $I(Y; T)$ on convolutional layer is closely equal to $H(Y)$.

For final output layer, the starting value of $I(X; T)$ and $I(Y; T)$ increase apparently with the expending of width. And also, with wider convolutional layer, the model reaches the upper bound faster. So wide CNNs can perform better with less training epochs. Specifically, in panel (c) and (d), we observe larger maximum value of $I(Y; T)$ for final output layer with increasing of width. Based on these observations, we believe that wide network is capable of capturing more information, which is beneficial to have better generalization.

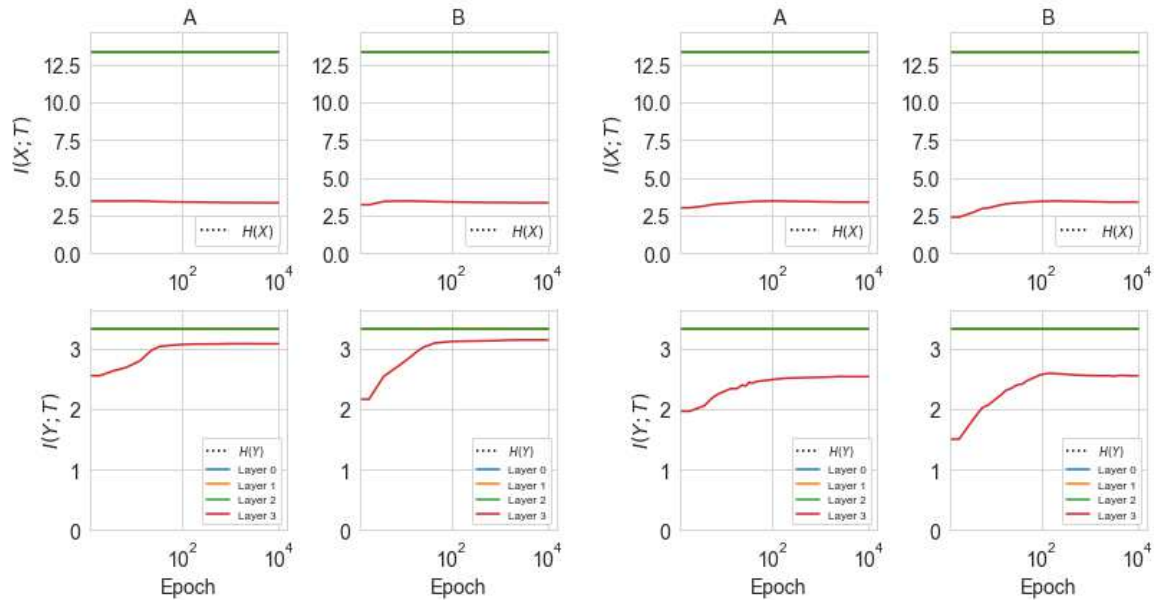
3.2 Kernel Size and Network Depth

Ref. [26] points out network with a large kernel size can be replaced by a deep network with small kernel size. From the perspective of information theory, how does the kernel size and depth affect MI in CNNs? We

¹ https://github.com/mrjunjieli/IB_ON_CNN



(a) MI on training data of MNIST. (A) without pooling layer (b) MI on training data of Fashion-MNIST. (A) without pooling layer (B) with pooling layer



(c) MI on test data of MNIST. (A) without pooling layer (d) MI on test data of Fashion-MNIST. (A) without pooling layer (B) with pooling layer

Fig. 7 (Colored online) MI path on CNNs with pooling layer. The width of all convolutional layers are 12-12-12 and the kernel size is fixed to 3x3. Moreover, the MaxPooling2D layer is added after the layer 1 and the pooling size is 2x2.

evaluate MI with various choices of depth and kernel size. By comparing information paths in Fig. 5 and Fig. 6, we find that both larger kernel size and deeper network can promote the starting value of $I(X; T)$ and $I(Y; T)$ on the final output layer, which implies network capture more information with less training. However, if we continuously increase kernel size or depth, the starting point cannot increase anymore or even becomes worse. So we propose that the larger kernel size and depth can drive network capturing more information with less training epochs. But over-large kernel size and depth will need more training epochs to capture the same amount of information. Furthermore, unlike convolutional layer width, in Fig. 5 (e), (f), (g), (h) as well as in Fig. 6 (c) and (d), we observe that they all reach the same maximum value of MI for final output layer, which

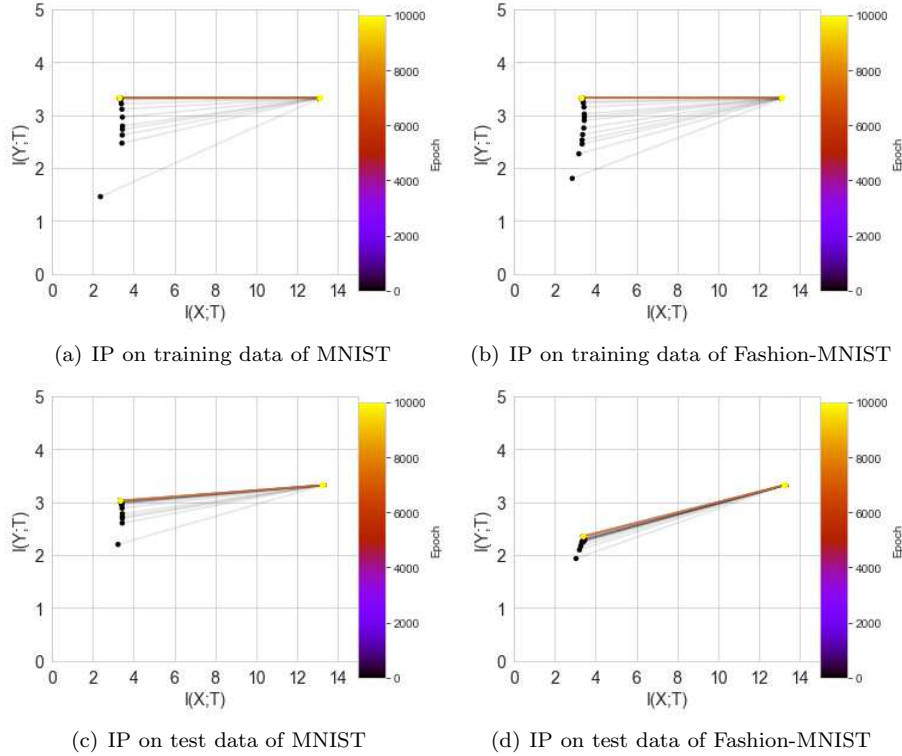


Fig. 8 Information plane for multi-fully connected layers on CNNs.

implies that a small kernel size and shallow depth are good enough to have a better generalization performance in these simple cases.

3.3 Pooling Layers and Multi-Fully Connected Layers

CNNs almost always include some forms of pooling layer such as max pooling and average pooling etc. The pooling layer always discards parts of data in order to improve the generalization and reduce computational complexity. In order to investigate the role of the pooling layer, we take the max pooling as example. In Fig. 7, we observe that the curves of MI grow in different ways. Panel (c) and (d) show the networks with pooling layer reach a little bit larger value than networks without pooling layer, which implies that pooling layer is beneficial to have better generalization.

We also design different CNNs with multi-fully connected layers to study whether double-sided saturating nonlinearities like *tanh* yield compression phase in CNNs. (Ref. [20] propose that double-sided saturating nonlinearities yield a compression phase while linear activation function can not). So, we use a network with 5 convolutional layers (convolutional layer width=3-3-3-3-3 and kernel size=3-3-3-3-3) and 4 fully connected layers (500-1024-500-10). Fig. 8 shows these layers information plane (IP) paths. From this we observe that all convolutional layers and fully connected layers (except for final output fully connected layers) converge to a point. In addition, the MI of final output layers grow during both training phase and test phase. So, we observe there are no compression phase occurs in the CNNs.

4 Conclusion and future works

Information bottleneck theory provides a interesting analytic tool to explore the inner behavior of deep neural network, and based on this, people try to understand why deep learning works well. Along this way, this paper tries to extend the study to CNNs and investigate how the fundamental features have impact on the performance of CNNs. Based on our cases, we summarize some key observations and draw conclusions as:

1. Convolutional layers can capture almost all information on input towards label. The MI between convolutional layers and input/output keep close to their upper bound.

2. Wide convolutional layers network is able to improve the generalization performance. Furthermore, wide network need less training epochs to reach its optimal performance than narrow one.

3. In general case, larger kernel size and deeper architecture drive network capturing more information with less training epochs. But, an over-large kernel size and over deep architecture will need much more training epochs to capture the same amount of information. This implies that people should balance the kernel size and network depth while design the deep architecture. Furthermore, it shows us the extremely deep neural network is probably not the right way to do deep learning.

4. In some simple cases, our results also reveal that there is no compression whether in convolutional layers or fully connected layers, even using double-sided saturating nonlinearities in CNNs. Hence, we tend to think the compression probably happen in some specific cases, but not a universal mechanism in deep learning, and further, the relationship between it and generalization needs more experimental verification.

In the future work, we plan to verify the above conclusions on some more complicated datasets such as ImageNet, and on some more complicated deep architectures such as Generative Adversarial Networks (GANs). We believe it will provide more experimental evidence to verify the IB theory and help us to understand deep learning.

Acknowledgements Our research is supported by the Tianjin Natural Science Foundation of China (20JCYBJC00500), the Science & Technology Development Fund of Tianjin Education Commission for Higher Education (2018KJ217).

References

1. Advani, M.S., Saxe, A.M.: High-dimensional dynamics of generalization error in neural networks. arXiv preprint arXiv:1710.03667 (2017)
2. Amjad, R.A., Geiger, B.C.: Learning representations for neural network-based classification using the information bottleneck principle. *IEEE Transactions on Pattern Analysis and Machine Intelligence* (2019)
3. Chechik, G., Globerson, A., Tishby, N., Weiss, Y.: Information bottleneck for gaussian variables. *Journal of machine learning research* **6**(Jan), 165–188 (2005)
4. Dai, B., Zhu, C., Wipf, D.: Compressing neural networks using the variational information bottleneck. arXiv preprint arXiv:1802.10399 (2018)
5. Elidan, G., Friedman, N.: Learning hidden variable networks: The information bottleneck approach. *Journal of Machine Learning Research* **6**(Jan), 81–127 (2005)
6. Friedman, N., Mosenzon, O., Slonim, N., Tishby, N.: Multivariate information bottleneck. arXiv preprint arXiv:1301.2270 (2013)
7. Gabrié, M., Manoel, A., Luneau, C., Macris, N., Krzakala, F., Zdeborová, L., et al.: Entropy and mutual information in models of deep neural networks. In: *Advances in Neural Information Processing Systems*, pp. 1821–1831 (2018)
8. Goldfeld, Z., Berg, E.v.d., Greenewald, K., Melnyk, I., Nguyen, N., Kingsbury, B., Polyanskiy, Y.: Estimating information flow in deep neural networks. arXiv preprint arXiv:1810.05728 (2018)
9. Goldfeld, Z., Van Den Berg, E., Greenewald, K., Melnyk, I., Nguyen, N., Kingsbury, B., Polyanskiy, Y.: Estimating information flow in deep neural networks. In: *Proceedings of the 36th International Conference on Machine Learning*, vol. 97, pp. 2299–2308 (2019)
10. Goodfellow, I., Bengio, Y., Courville, A.: *Deep learning*. MIT press (2016)
11. Guidotti, R., Monreale, A., Ruggieri, S., Turini, F., Giannotti, F., Pedreschi, D.: A survey of methods for explaining black box models. *ACM computing surveys (CSUR)* **51**(5), 93 (2019)
12. Hsu, W.H., Kennedy, L.S., Chang, S.F.: Video search reranking via information bottleneck principle. In: *Proceedings of the 14th ACM international conference on Multimedia*, pp. 35–44 (2006)
13. Jónsson, H., Cherubini, G., Eleftheriou, E.: Convergence of dnns with mutual-information-based regularization. *Proc. Bayesian Deep Learning@ Advances in Neural Information Processing Systems (NeurIPS)*, Vancouver (2019)
14. Kadmon, J., Sompolinsky, H.: Optimal architectures in a solvable model of deep networks. In: *Advances in Neural Information Processing Systems*, pp. 4781–4789 (2016)
15. Kolchinsky, A., Tracey, B.: Estimating mixture entropy with pairwise distances. *Entropy* **19**(7), 361 (2017)
16. Kolchinsky, A., Tracey, B.D., Wolpert, D.H.: Nonlinear information bottleneck. *Entropy* **21**(12), 1181 (2019)
17. Krizhevsky, A., Hinton, G., et al.: Learning multiple layers of features from tiny images (2009)

18. Painsky, A., Tishby, N.: Gaussian lower bound for the information bottleneck limit. *The Journal of Machine Learning Research* **18**(1), 7908–7936 (2017)
19. Poole, B., Ozair, S., Oord, A.v.d., Alemi, A.A., Tucker, G.: On variational bounds of mutual information. arXiv preprint arXiv:1905.06922 (2019)
20. Saxe, A.M., Bansal, Y., Dapello, J., Advani, M., Kolchinsky, A., Tracey, B.D., Cox, D.D.: On the information bottleneck theory of deep learning. *Journal of Statistical Mechanics: Theory and Experiment* **2019**(12), 124020 (2019)
21. Saxe, A.M., McClelland, J.L., Ganguli, S.: Exact solutions to the nonlinear dynamics of learning in deep linear neural network. In: *International Conference on Learning Representations*. Citeseer (2014)
22. Shamir, O., Sabato, S., Tishby, N.: Learning and generalization with the information bottleneck. *Theoretical Computer Science* **411**(29-30), 2696–2711 (2010)
23. Shwartz-Ziv, R., Tishby, N.: Opening the black box of deep neural networks via information. arXiv preprint arXiv:1703.00810 (2017)
24. Slonim, N., Tishby, N.: Document clustering using word clusters via the information bottleneck method. In: *Proceedings of the 23rd annual international ACM SIGIR conference on Research and development in information retrieval*, pp. 208–215 (2000)
25. Strouse, D., Schwab, D.J.: The deterministic information bottleneck. *Neural computation* **29**(6), 1611–1630 (2017)
26. Szegedy, C., Vanhoucke, V., Ioffe, S., Shlens, J., Wojna, Z.: Rethinking the inception architecture for computer vision. In: *Proceedings of the IEEE conference on computer vision and pattern recognition*, pp. 2818–2826 (2016)
27. TISHBY, N.: The information bottleneck method. *Computing Research Repository (CoRR)* (2000)
28. Tishby, N., Zaslavsky, N.: Deep learning and the information bottleneck principle. In: *2015 IEEE Information Theory Workshop (ITW)*, pp. 1–5. IEEE (2015)
29. Wang, Q., Gao, J., Li, X.: Weakly supervised adversarial domain adaptation for semantic segmentation in urban scenes. *IEEE Transactions on Image Processing* **28**(9), 4376–4386 (2019)
30. Wang, Q., Yuan, Z., Du, Q., Li, X.: Getnet: A general end-to-end 2-d cnn framework for hyperspectral image change detection. *IEEE Transactions on Geoscience and Remote Sensing* **57**(1), 3–13 (2018)
31. Yu, S., Principe, J.C.: Understanding autoencoders with information theoretic concepts. *Neural Networks* **117**, 104–123 (2019)
32. Yu, S., Wickstrøm, K., Jenssen, R., Principe, J.C.: Understanding convolutional neural networks with information theory: An initial exploration. *IEEE Transactions on Neural Networks and Learning Systems* (2020)
33. Yu, Y., Chan, K.H.R., You, C., Song, C., Ma, Y.: Learning diverse and discriminative representations via the principle of maximal coding rate reduction. arXiv preprint arXiv:2006.08558 (2020)

5 Appendix

In order to further verify our conclusions, we conduct additional experiments on the CIFAR-10 dataset [17]. This dataset consists of 60,000 32x32 colour images in 10 classes, with 6,000 images per class. There are 50,000 training images and 10,000 test images.

In this experiment, the whole **50,000** training images and 10,000 test images are selected as our training dataset and test dataset respectively, which is the only different setting from *Experiments and discussion* section. Furthermore, because of the arithmetic of computing mutual information, we choose to average the image of three channels and turn it into a signal channel as input data.

The Fig. 9 and Fig. 10 show the MI with different widths and depths on training data respectively. Fig. 11 shows the MI with pooling layer on test data. These results offer more proof about the IB theory.

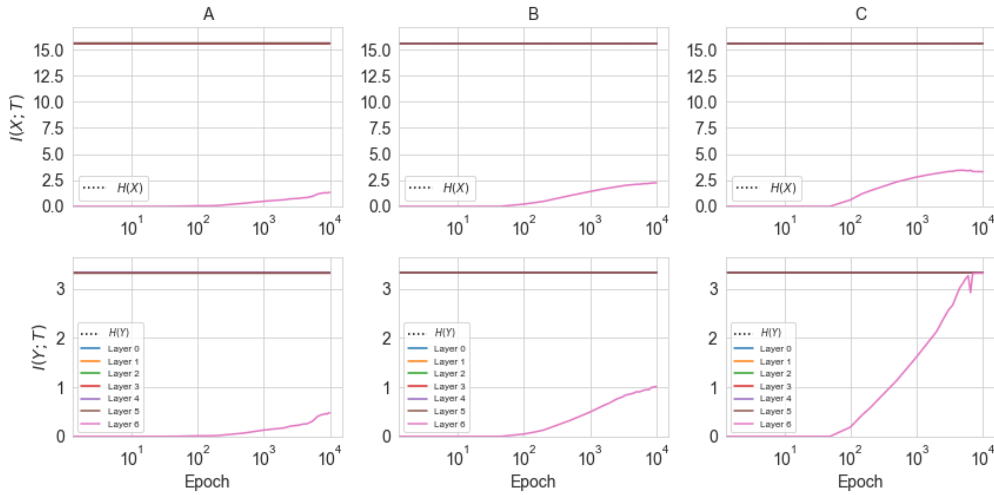


Fig. 9 (Colored online) MI path on CNNs with different convolutional layer widths on training data of CIFAR-10. The convolutional layer width of 3 networks are (A) 3-3-3-3-3-3 (B) 6-6-6-6-6-6 (C) 12-12-12-12-12-12.

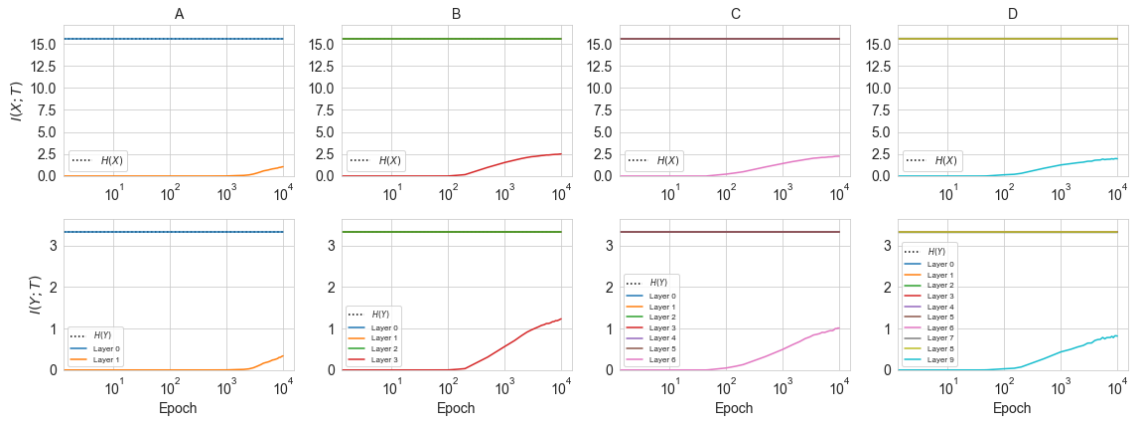


Fig. 10 (Colored online) MI path on CNNs with different convolutional layer depths on training data of CIFAR-10. The depth of 4 networks are (A) depth=2 (B) depth=4 (C) depth=7 (D) depth=10. All these networks width are set to 6.

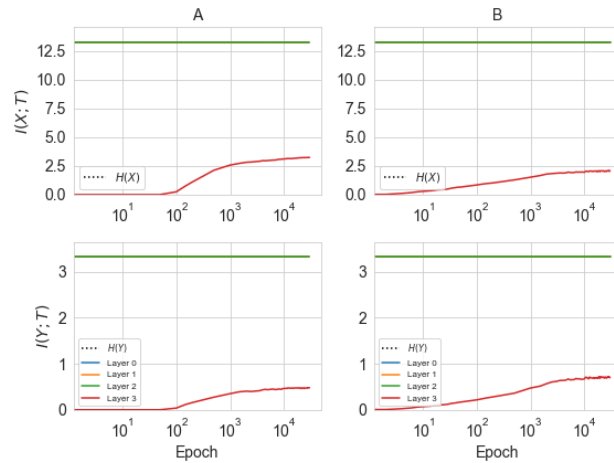


Fig. 11 (Colored online) MI path on CNNs with pooling layer on test data of CIFAR-10. (A) without pooling layer (B) with pooling layer. The width of convolutional layers are both 6-6-6 and the kernel size is fixed to 3x3. Moreover, the MaxPooling2D layer is added after the layer 1 and the pooling size is set to 2x2.